

NMR-Based Water Saturation Estimates in Ekofisk Waterflood Zones

J. Howard, H. Hermansen, A. Vedvik

Phillips Petroleum Company, Norway; Phillips Petroleum Company, USA

Abstract

Non-Archie-based water saturation estimates are important in Ekofisk water breakthrough zones because of uncertainty related to water resistivity (R_w) and Archie equation parameters. Many traditional non-Archie methods such as C/O logs are limited in their use at Ekofisk because of the lack of calibration opportunities. In contrast, NMR logging measurements require minimal calibration and produce a signal that can be interpreted with a simple physical model. The shallow depth of investigation of current NMR logging tools makes this measurement comparable to flushed zone saturation. Water saturation estimated from NMR logs at Ekofisk generally are in agreement with flushed-zone saturation obtained from shallow resistivity tools and an imbibition-based interpretation model. Saturation exponents extracted from the NMR-based saturation are in agreement with the laboratory imbibition values for most of the Ekofisk and Tor formations. The NMR-based values provide more reasonable results in the less water-wet Upper Ekofisk formation. The NMR-based interpretation model is easier to apply since it requires fewer unknowns as inputs. NMR response is not influenced by the most difficult parameter for resistivity models, the water salinity in a mixed formation/waterflood region.

Introduction

The new generation of Nuclear Magnetic Resonance (NMR) logging tools has made significant contributions to a wide range of formation evaluation topics since it was introduced in the early 1990's (Kenyon, 1997; Coates *et al.*, 1999). The combination of stable permanent magnets that can survive the borehole environment, more sophisticated electronics that allow for pulsed-experiments, and recent innovations in signal processing has lead to a powerful petrophysics tool. Logging NMR measurements focus on quantifying the abundance of protons in the fluid phases and the nature of the interactions between these fluids and the pore walls. The advantage of NMR measurements is that besides its obvious role as a porosity tool, it has the ability to apportion the porosity into different components. The connection between these different, sometimes easily recognizable relaxation components is a matter for the interpretation models. The same relaxation time distribution can be interpreted with pore size variations in mind, or in other cases differences in fluid types, e.g. water versus hydrocarbons of varying viscosities. The most common application is the determination of formation permeability based on a simple model of combined pore sizes. Matrix permeability in the Ekofisk chalk is of less interest to reservoir management teams, instead there is a greater need to understand fluid saturations in zones where conventional interpretation efforts are constrained.

A concern was raised during a study of residual oil saturation in Ekofisk Field whether saturation exponents determined from core analyses at imbibition endpoints (S_{wf}) are sufficient and proper for use in standard water saturation calculations in the flushed zone (S_{xo})

or in waterflooded intervals. Available laboratory data indicate that resistivity hysteresis occurs between the drainage and imbibition endpoints, thereby complicating the determination of the saturation exponent used in the Archie water saturation model. A resolution of this question was hampered by the lack of core results at forced displacement endpoints (S_{wff}). The basis of this combined laboratory and field study is that water saturation measurements obtained from shallow-reading NMR logging tools can be used to optimize core-derived saturation exponents that are used in waterflooded intervals of the Ekofisk Field. A key aspect of this study is the use of field-based data to resolve differences in parameter selection for the standard water saturation calculations from resistivity logs.

Data

Four wells in the Ekofisk Field were logged since 1994 with Numar's NMR logging tool, the MRIL-C. Three of those wells, 2/4K-08A, 2/4X-08 and 2/4K-11A were drilled with water-based muds, which has the desired consequence of having a micro-resistivity (R_{xo}) measurement as part of the data package. These three wells were used for the evaluation of the NMR-derived saturation exponent. The logging jobs for these wells differ in the specifics of the tool setup. In general the more recent wells, such as the 2/4K-11A and 2/4X-08, have more favorable operating parameters for NMR interpretation. The time span between these logging jobs is important since unlike most logging tools after their initial release the NMR technology continued to develop, both in improvements in the tool's response and with interpretation methodologies (Table 1).

Table 1. NMR logs on Ekofisk Waterflood Intervals.

Well	Date	Logging Speed (ft/min)	Number Echoes
2/4K-08A	August 1995	3-5	150
2/4-X08	January 1997	4-12	170 - 300
2/4-K11A	March 1998	5-6	700

The most significant improvement is in the number of CPMG spin echoes collected for each depth increment. This is a result of improved tool efficiency and the use of additional capacitor subs that supply sufficient power to the tool in order to collect longer echo trains. The increased length of the collected echo train is critical in generating useful and unambiguous relaxation time distributions for estimating water saturation.

The logging speed is strongly dependent upon the wait time chosen to ensure complete polarization of the fluid's protons. Given the slow relaxation of the hydrocarbon, the tool is set up with a slow wait time, 6 to 8 seconds. For this reason logging speeds with the MRIL-C tool have not improved over the years. The newer generation NMR logging tools that have pre-polarization magnets should, however, be able to run at significantly faster speeds with no loss of data quality. These tools simply have additional magnets that extend beyond of the transmitter/receiver coil and are effective in polarizing the fluid protons before the tool moves into measurement range.

The MRIL-C tool has sufficient signal/noise levels in the high porosity Ekofisk Field chinks that makes it possible to evaluate water saturations quantitatively. The two K-wells were drilled as replacements for nearby injector wells, such that water saturations throughout most of the reservoir interval approach end point values. The X-well example comes from a standard reservoir interval at initial water saturation. Any measured increase in saturation is due solely to mud filtrate invasion. In all wells the NMR tool should have a depth of investigation that is comparable to the micro-resistivity tool that is the basis of S_{xo} estimates.

Operations

Several special calibration steps are required when running NMR logs in waterflood zones compared to conventional reservoir intervals. Porosity calibration is the most important, and it is more challenging since it is not as intuitive as one might expect upon first inspection. The signal intensity that a NMR tool measures is directly scaled into porosity units in real time at the well site. The scaling factors are determined by calibration measurements made in the shop and on the rig floor. The tool measures the magnitude of the magnetic field associated with the fluid protons in the tool's sensitive region. This intensity is strongly dependent upon the temperature of the protons themselves. Therefore in addition to the standard tool temperature corrections that are made with sonde sensors the porosity is also corrected to account for the reduced temperatures in the waterflooded formation. Borehole temperatures measured during logging runs can be dramatically different than the temperature of the actual waterflooded interval, with differences up to 40°C at Ekofisk Field (Van De Verg *et al.*, 1999).

The choice of formation temperature creates a slight change in porosity based on Curie Law behavior,

$$M_o \propto N/kT$$

Where M_o is the measured signal intensity or magnetization, N is the number of protons or spins present, k is the Boltzmann constant and T is the temperature in °K. Given that Nk is constant, this would suggest that the measured signal intensity is inversely proportional to temperature, so that lower temperatures should lead to a higher signal intensity or porosity.

Lower temperatures measured in the cased-hole several weeks after open-hole logging are commonly observed in waterflooded intervals (Van De Verg *et al.*, 1999). It appears to be counter-intuitive, but a lower temperature results in lower calculated porosity (Figure 1). This occurs even though the lower temperature for a given number of protons produces a slightly higher signal magnitude and apparent NMR porosity as indicated in the Curie Law. The apparent porosity, however, has to be calibrated against the calibration tank porosity (100% at room temperature). It is this adjustment that causes the estimated NMR porosity at reduced cased-hole temperatures to be lower than if calculated with open-hole temperatures. The key step in this analysis is the calibration of measured signal intensity against a porosity standard. The calibration tank apparent porosity follows Curie Law behavior, e.g. decreases at higher temperatures, but the measured logging tool voltages have to be matched to this calibration curve.

The light hydrocarbon at Ekofisk, also requires sufficient time to polarize all its protons. This long wait time is responsible for the slow logging speeds. Pulse sequences that take advantage of the significantly different polarization times for the two fluids, however, do not appear to be very helpful at Ekofisk. Earlier versions of the logging tools required multiple passes to collect data with different wait times. The difficulty in depth-matching these passes is magnified by the need to merge echo trains before inversion. Cooler formation temperatures shift the hydrocarbon signal towards faster relaxation times, increasing the chances for overlap of the two fluid responses. In these cases a more robust model of that accounts for a broader hydrocarbon signal is required to separate the water contribution.

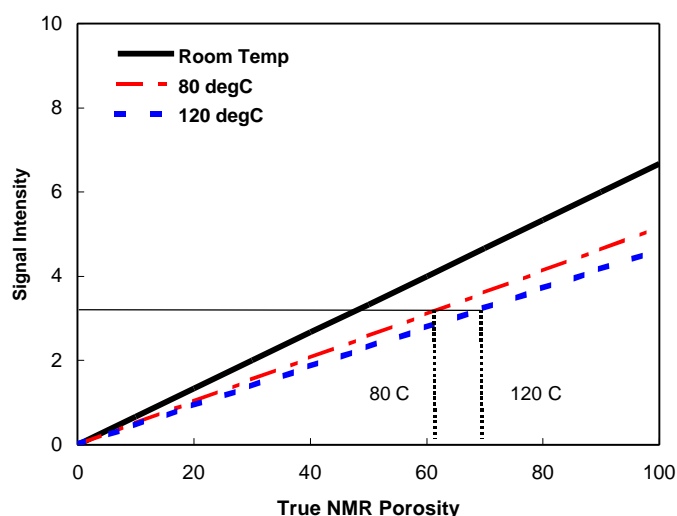


Figure 1. MRIL temperature calibration plot illustrates effect of different formation temperatures on interpreted porosity from measured signal intensity. Curie Law behavior is observed at 100% porosity where higher temperature measurements have reduced signal intensity. Measured signal intensity or apparent porosity reads closer to “true” porosity as temperatures approach the original room calibration temperature.

Results

Laboratory Calibration

The log interpretation models are based on a large collection of laboratory measurements that illustrate how the relaxation time distributions can provide quantitative information about porosity and saturation. Laboratory NMR measurements do an excellent job of determining all of the available porosity in chalks as measured by conventional core methods (Howard and Spinler, 1995). There is no loss of porosity due to fluid located in pores that are too small to be detected by NMR relaxation methods. Contrast this with conventional petrography and image analysis of thin section micrographs where most of the pores are not detected. The calibration of NMR porosity methods is based simply on the relationship between the number of protons in the pore volume and the measured signal intensity.

Relaxation time distributions for water-saturated chalk samples are narrow single peaks, which suggest unimodal pore-size distributions (Howard *et al.*, 1994). There are some variations based upon lithology and mineralogy. The better reservoir lithologies, i.e. the non-laminated types, tend to have slower relaxation times that suggest slightly larger pores. For chalks with the same pore size, samples from the Tor Formation tend to have slightly slower relaxation times than Ekofisk Formation samples. The Tor samples have less clay mineral and other non-calcite phases that tend to enhance relaxation processes. A generalization is that water in chalk pores has relaxation times less than 200 milliseconds, the actual value determined by pore size and the amount of non-chalk lithology present.

Immiscible mixtures of oil and water in chalk are readily studied by laboratory NMR measurements (Howard, 1998). Water saturation estimates from NMR measurements are based on the observation that chalk samples have distinct relaxation time properties for the water and hydrocarbon fluid phases. In part the distinctiveness of these measured distributions is due to the unimodal pore-sizes found in chalks. The relaxation peak associated with the water fraction in chalk is found between 10 and 150 milliseconds, depending in part upon pore-size, wettability and saturation. In contrast, low viscosity oil, such as found in the Ekofisk reservoir, has a relaxation time slower than 200 milliseconds, regardless of amount of the non-wetting phase or wettability. The laboratory results indicate that a simple cutoff time

of around 150-200 milliseconds would be sufficient to distinguish between oil and water relaxation components.

Laboratory experiments often have experiment lengths of several seconds, making resolution of these two components very straightforward. This example of a water-wet chalk shows how the relaxation component associated with the water shifts towards slower times and increases in intensity as water content changes from initial saturation (S_{wi}) of 0.15 to an imbibition endpoint (S_{wf}) of 0.70 (Figure 2). The shift in relaxation time corresponds to a thickening of the water layer around each pore, essentially an increase in effective water-filled pore size. The slow relaxation time component associated with the light oil only decreases in intensity during the course of water imbibition. The relaxation time of 1.3 to 1.5 seconds corresponds to the bulk relaxation time for this oil. The absence of a relaxation time shift in this sample indicates the lack of interactions between the oil and the pore walls. This sample therefore is highly water-wet. In contrast, less water-wet samples are characterized by shifts in the oil relaxation component towards faster times, sometimes faster than 500 milliseconds.

Quantitative estimates of water saturation at different stages of the imbibition process are generated simply by integrating the area under each relaxation mode. The comparison between NMR-based values and standard weight-based values indicates the robustness of the NMR technique (Figure 3). Measurements at initial and imbibition endpoint saturation show good correlation throughout the saturation range. There are no corrections necessary for the NMR measurements beyond a simple Hydrogen Index correction for oil. Hydrogen Index is defined as the ratio of the proton density of the fluid relative to the proton density of pure water. The oil has a Hydrogen Index that is within 3% of that for pure water, so that the intensity corrections to the relaxation time distributions are small. The experience in this lab is that the NMR results for water saturation tend to be more accurate since they are less sensitive to sample weight loss that often accompanies standard core handling.

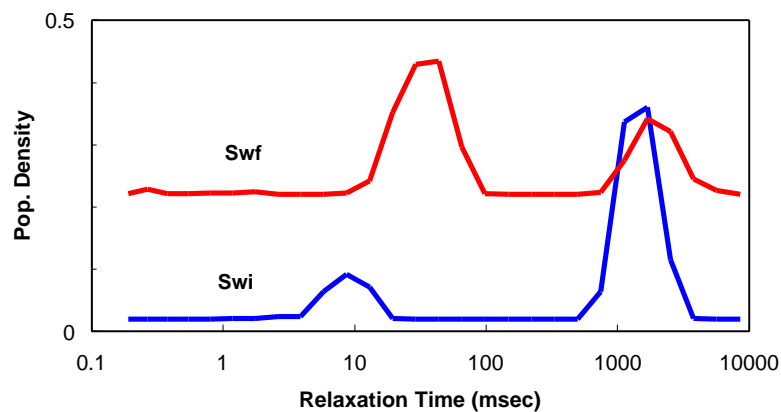


Figure 2. Laboratory NMR relaxation time distributions of chalk at partial oil-water saturation. Initial water saturation (S_{wi}) shows small component at fast times for water that increases in intensity and shifts to slower times during imbibition (S_{wf}).

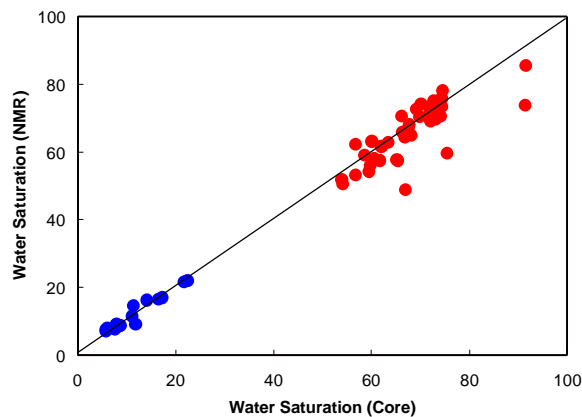


Figure 3. Comparison of water saturation estimates from conventional core methods and laboratory NMR measurements of relaxation time distributions. Measurements made at initial water saturation (blue) and at imbibition endpoint (red).

The difficulty in applying this approach of identifying the individual relaxation components to the log results at Ekofisk Field is that the experiment time for each NMR pulse sequence can be as short as 360 milliseconds or less. The number of collected echoes times the echo spacing, 1.2 milliseconds for the MRIL-C tool defines the experiment length. While the proton contribution from slower relaxing components is measured in the overall signal amplitude, the ability of the processing techniques to resolve and characterize relaxation components that are slower than the experiment length is severely limited. The inversion of the raw echo train data into relaxation time distributions reveals a dominant single relaxation component throughout most of the interval. There are some intervals in these earlier wells where a distinct bimodal distribution is detected.

We have done some numerical and laboratory experiments to determine the effect that limited experiment lengths have on the results of the mathematical inversion process. These results support our interpretation that the two relaxation components tend to be combined into a single mode. A chalk sample containing approximately 60% water and 40% decane, a low viscosity hydrocarbon with a T_2 of 1500 milliseconds at room temperature, was measured in a desktop 2.0 MHz spectrometer under varying sampling parameters. The echo spacing was kept constant at 1.2 milliseconds, a polarization time of 8 seconds was used to ensure complete polarization and only 2 echo trains were collected in order to mimic logging data acquisition. A base measurement of 4096 echoes was established, followed by shorter echo trains consisting of 500, 300 and 150 echoes. The raw data was inverted with the standard inversion algorithm, using a time constant basis function of 16 points spaced between 3 and 3000 milliseconds. The baseline measurement of 4096 echoes with its experiment length of 4900 milliseconds, is characterized by two relaxation components. The water phase is found at 50 milliseconds and the slower hydrocarbon component at 600 milliseconds. The shift in the slow components towards faster times suggests that the sample is less water-wet than other laboratory samples. For more water-wet samples the effect on relaxation time distributions would be even more pronounced than in this example. As the experiment length decreases, as determined by the number of collected echoes, the relaxation time distributions are altered by a loss of the slow relaxation component (Figure 4). When the experiment length is reduced to 150 echoes, the relaxation time distribution is characterized by a single mode centered at 50 milliseconds but with a more pronounced tail at slower times.

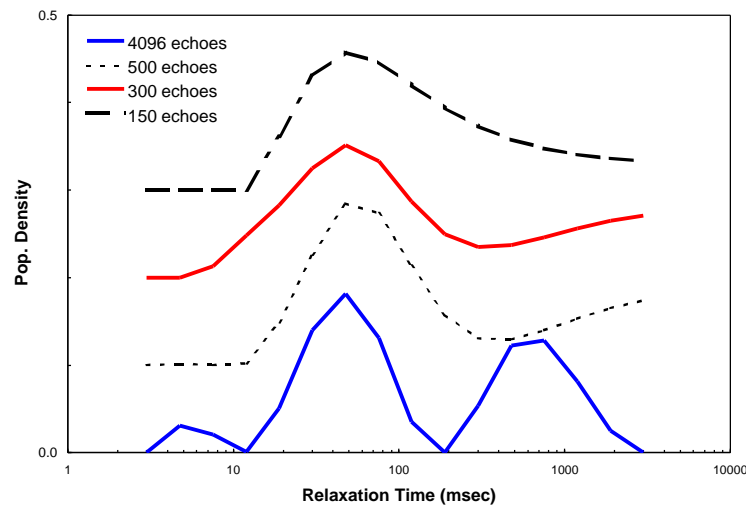


Figure 4. Effect of reduced experiment length on relaxation time distribution. Original data of 4096 echoes is truncated to match output from NMR logs. Conventional processing methods result in broad unimodal distributions.

The later wells are characterized by echo trains that contain experiment lengths of 500 or more milliseconds that have sufficient information to reveal distinct bimodal distributions. Even with the better quality data it is often necessary to use a more robust inversion technique than what is generally provided by the service companies at well site.

It is important to acknowledge that the available inversion techniques used to transform echo decay curves to relaxation time distributions are quite robust and are capable of finding a solution for time constants where there is not accompanying data. For example, the multiple component function that is solved in this transformation consists of a series of single-exponential terms characterized by pre-assigned first-order rate constants; T_2 values. It is not uncommon to create a basis function of these rate constants that span several orders of time magnitude. The standard MRIL processing consists of 8 to 10 time components ranging from 4 to 1024 milliseconds spaced in powers of 2. Very clearly, the inversion algorithm is assigning population density contributions to time constants that extend beyond the length of the actual echo-train experiment, only 360 milliseconds in the earlier wells. While this is mathematically permissible, one does have to be concerned about the physical implications of some of these solutions.

At the same time the inversion process must deal with less than ideal signal-to-noise levels in the data. The smoothing or regularization term is often set high in order to produce a stable solution on a depth-by-depth basis. Too much smoothing, however reduces the relaxation time distribution to a broad, single-mode component that is difficult to interpret. Much of our success with the interpretation of Ekofisk MRIL logs results from the reprocessing of the data with a reduced smoothing function (Figure 5). This example from a waterflooded interval in the Upper Ekofisk section of the 2/4K-11A illustrates the richness of information that can be extracted from NMR log data. Hints of the bimodal character of the data are observed in the service-company results. Inversion with more time constants generates a distinctly bimodal distribution. The new distribution generates a total porosity that matches conventional porosity. The interpretation of water saturation is also simpler with the new distribution and shows good agreement with standard S_{x_0} estimates.

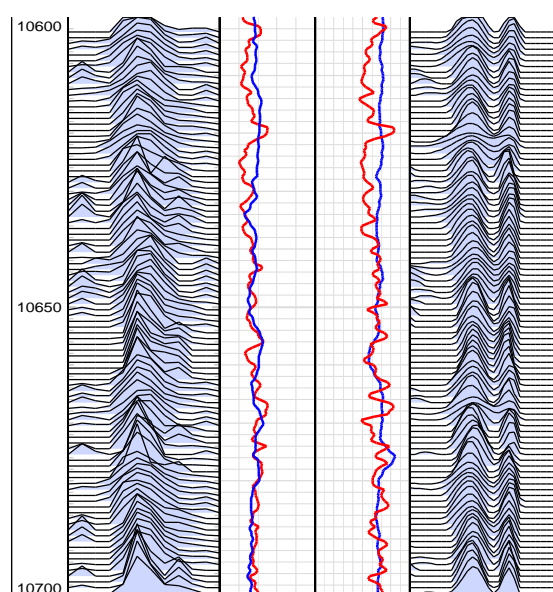


Figure 5. Comparison of relaxation time distributions generated by service company processing (left) and in-house (right). NMR-derived porosity (blue – 2nd track) and water saturation (blue – 3rd track) compare favorably with conventional results (red).

Porosity

The results from the earlier logged wells are more difficult to evaluate. The first concern is whether the tool actually detected all of the fluids. Given the absence of the bimodal distribution, it is not clear what phase the recorded distribution most likely represents. There is the possibility that only the fast relaxation components are detected and that the single mode corresponds only to the water phase.

NMR log porosity closely approximates other estimates of total porosity in the reservoir, e.g. density logs (Figure 6). This suggests that all of the pore fluid is measured by the NMR experiment. Porosity is determined by one of two methods. The first method extrapolates the echo decay curve back to an initial time of 0 milliseconds, while the second method integrates the area under the relaxation time distribution. Since the porosity from both methods captures most of the available fluid signal, it appears that the relaxation time distribution contains porosity information from both water and hydrocarbon phases.

Since the single relaxation mode contains most of the total porosity, the most logical interpretation is that the very slow relaxation associated with the hydrocarbon is combined with the more easily resolved water relaxation. This interpretation therefore makes it more difficult to estimate water saturation from the standard method of measuring the relative population density of protons associated with each relaxation mode.

The ability of NMR logging tools to measure the total porosity is more dependent upon the wait time rather than the number of collected echoes. The earliest logging jobs at Ekofisk have good porosity matchups through most of the reservoir, including the waterflooded intervals. NMR porosity is lower than conventional log porosity in a few zones in these earlier wells because of incomplete polarization of the slow relaxation components (Figure 7). This interval from the 2/4K-08A is at non-waterflood conditions and contains a low viscosity oil in a highly water wet system. Insufficient wait time reduces the contribution of the oil to the total porosity.

A log example from the more recent 2/4K-11A in the Tor formation illustrates that proper tool setup that uses a slow wait time results in a good porosity match between NMR and conventional logs (Figure 8).

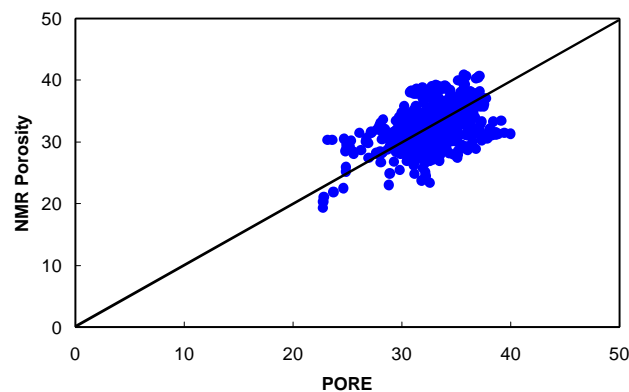


Figure 6. Comparison of NMR log porosity and conventional log porosity for the waterflooded intervals of the 2/4K-11A well.

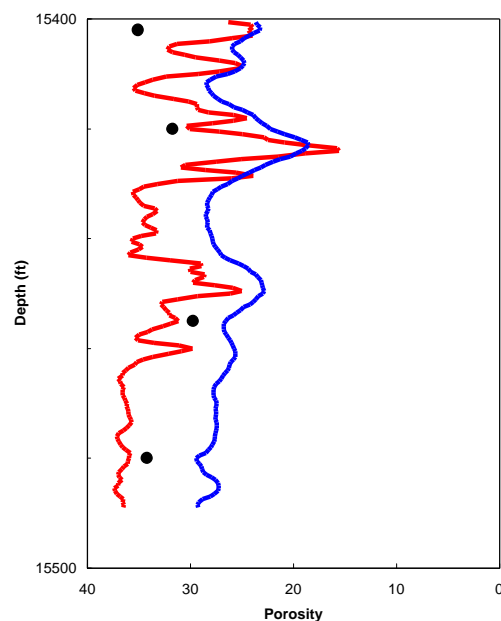


Figure 7. Incomplete polarization of hydrocarbon in Tor section of 2/4K-08A results in reduced NMR porosity (blue) compared to conventional (Red). Several core points confirm the NMR logs loss of porosity.

Two key points to make. The first is that as the number of echoes decreases, the ability of the processing algorithms to resolve slow relaxation components also decreases. The area under the curve that corresponds to total porosity remains constant. The second factor is that while the slow hydrocarbon peak is being adsorbed into the faster relaxing water peak, there is no significant shift in the time of this component. The implication is that the relaxation times associated with the water peak and used for pore size and wettability determinations are not altered significantly.

Water Saturation

Water saturation was estimated from the NMR relaxation time distributions for the three wells. Only those intervals with good hole quality and where NMR-derived porosity matched density-based effective porosity were used. The porosity match ensures that the NMR measurement included full polarization of all of the available protons, which in turn ensures that the relaxation time distribution is complete.

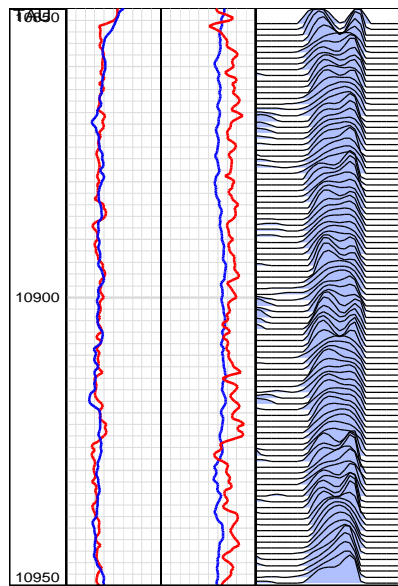


Figure 8. NMR log results from Tor Formation, 2/4K-11A. Porosity in the left track, NMR (blue) and conventional (red) show good agreement.

Estimating water saturation from NMR log data is more difficult when the relaxation time distributions are characterized by a single broad mode. The choice of a cutoff time to distinguish water from the oil is based in part on laboratory results and from log data in predominantly water zones such as the EE layer or Tight Zone. At the time the selection of cutoff time seemed arbitrary at best, but the results from better quality data from more recent wells tends to confirm the original approach (Figure 5 and 9). In these 2/4K-11A examples the bimodal nature of the relaxation time distribution is clearly recognizable. The separation of water and oil relaxation components is done with a simple cutoff time that can be adjusted for each zone by visual inspection. It is interesting to note the difference in relaxation behavior in this well between the EC and ED layers. There appears to be a distinct change in the water relaxation time even though the total water saturation remains constant. The relaxation time distribution shifts towards faster times along with a much reduced oil component in the EE layer. The faster times suggest smaller pores and/or a greater abundance of non-carbonate grain coatings in this particular non-reservoir lithology. The porosity matchup in the left track of Figure 9 is typical of NMR logs in the Ekofisk. Water saturation estimates in the middle track from NMR (blue) and S_{xo} (red) are in good agreement through much of this waterflooded interval. NMR estimates slightly lower water saturation values through part of the interval. The NMR results are also characterized by lower vertical resolution than the conventional logs. This results from both the large measurement aperture of the MRIL-C tool and data stacking in the processing steps.

A weighted average for each geological layer was calculated from the proportion of points (depth interval) for each well. Some layers were not logged in all of the wells so that the final average NMR-based saturation sometimes is the result of a small number of points. The NMR-derived saturation matches the standard Archie derived values in the Tor and Lower Ekofisk layers, but there are greater differences in the upper Ekofisk (Table 2). Greatest discrepancy occurs in the Upper Ekofisk layers where NMR-derived values exceed the S_{xo} from the same wells.

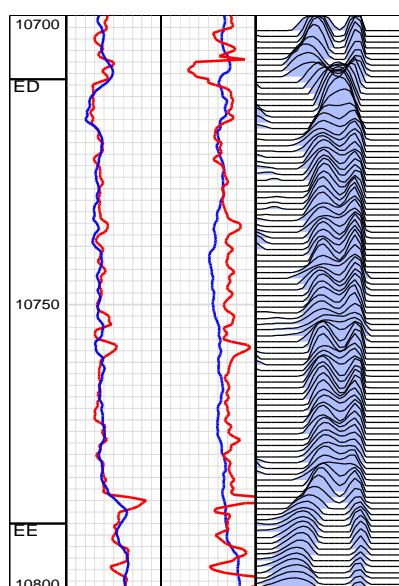


Figure 9. NMR log results from waterflooded ED layer in 2/4K-11A. Distinct bimodal relaxation time distributions enhance interpretation of NMR logs (blue) for porosity (left track) and water saturation (middle track). Note the different distribution for the EC layer at the top of the interval.

Table 2. Comparison of standard Archie-derived shallow water saturations and NMR-derived water saturations.

Layer	S_{xo}	S_w from NMR Logs
EA	68.8	72.5
EB	65.6	70.0
EC	64.4	72.9
ED	67.7	68.9
TA	69.6	70.6

Calculated Saturation Exponent

The saturation exponent, n , was determined from the Archie equation,

$$n = \frac{\log(S_w)}{\log(R_{xo}) / (aR_w / f^m)}$$

where S_w is the NMR-derived water saturation, R_{xo} is the micro-resistivity log value, Φ is the conventional log porosity, a and m are the Archie parameters determined from core analyses for each geological layer and R_w is the temperature-corrected resistivity of the mud filtrate. Temperature corrections for R_w , actually the R_{mf} of the mud filtrate, were done using the well-site temperature measurement of the filtrate and the borehole temperature curve measured during the micro-resistivity pass.

Continuous curves of saturation exponent were determined for the intervals in these three wells that had high quality NMR log results. An average saturation exponent for each geological layer was calculated from these continuous curves (Table 3). Intervals were evaluated to include only those sections with good borehole quality and a porosity match between NMR and conventional logs. An example of this evaluation is the EA layer in the 2/4X-08 well where borehole washout causes increased NMR porosity estimates, thereby invalidating the water-saturation estimates through most of this interval. The overall impact in this well was to reduce the number of valid sample points in the EA layer by more than half.

Table 3. Comparison of NMR-derived saturation exponent and average value determined from core analyses for different Ekofisk reservoir layers.

Layer	Core	NMR
EA	2.0	2.9
EB	2.0	2.6
EC	2.0	2.6
ED	2.3	2.2
TA	2.4	2.3

Table 4. Comparison NMR-log derived saturation exponents for Geological Layers and Breakthrough Zones.

Geological Layer	Saturation Exponent	Breakthrough Zone	Saturation Exponent
EA	2.6	WEA	2.6
EB	2.6	WEB	2.6
EC	2.6	WEC	2.7
ED	2.2	WED	2.4
TA	2.3	WTA	2.2

These NMR-derived saturation exponents are compared with those determined from the 1995 laboratory resistivity study where resistivity was measured at the imbibition end point for each sample. There is little laboratory data of resistivity measurements at forced displacement end points on Ekofisk cores.

The reduced number of NMR log sample points available for evaluation skews the Upper Ekofisk exponents. The saturation exponent for the EA layer contains points from a single well, 2/4X-08, of which approximately half of the entire interval is not considered because of poor data quality. If the entire Upper Ekofisk is considered as a single layer, then the weighted average NMR-derived saturation exponent from all three wells is 2.6. This average value takes into account the observation that much of the EA data is poor quality and should not be weighted as heavily as results from EB and EC layers.

NMR-derived saturation exponents were also tabulated for breakthrough intervals only in the two study wells that exhibit water breakthrough; 2/4K-08A, and 2/4K-11A. These breakthrough intervals were defined by a series of criteria such as formation temperature and have the overall effect of reducing the number of sample points per geological layer by roughly half. The difference in NMR-derived saturation exponents determined from geological and breakthrough layers is small (Table 4). The EA layer does not have any acceptable breakthrough zone data in the three study wells. An averaged value of 2.6 from all Upper Ekofisk breakthrough layers is suggested for the WEA layer.

The result of calculating Archie saturation exponents from NMR-log based water saturation estimates for flushed zone saturation evaluation is that an average value of 2.6 should be used in Upper Ekofisk intervals instead of the core-derived value of 2.0. This is an average of the combined results from EA, EB and EC layers, with less significance placed on the EA results because of data quality issues. The impact on S_{x_0} estimates in the Upper Ekofisk intervals is that NMR-based saturations are 6 to 10 saturation units greater than saturations determined with core-based Archie exponents. The effect upon Lower Ekofisk and Tor saturation estimates is minimal since the NMR-based exponents are similar to the core-derived values.

Conclusions

Water saturation estimated from NMR logs at Ekofisk generally are in agreement with flushed-zone saturation obtained from shallow resistivity tools and an imbibition-based interpretation model. Saturation exponents extracted from the NMR-based saturation are in

agreement with the laboratory imbibition values for most of the Ekofisk and Tor formations. The NMR-based values provide more reasonable results in the less water-wet Upper Ekofisk formation. The NMR-based interpretation model is easier to apply since it requires fewer unknowns as inputs. NMR response is not influenced by the most difficult parameter for resistivity models, the water salinity in a mixed formation/waterflood region.

The derivation of NMR-based saturation exponents depends largely upon how much confidence one places in the NMR-based saturations. While the physics of the measurement is very straightforward, there is an interpretation issue of how to separate the water and hydrocarbon phases at the reduced formation temperatures experienced in highly waterflooded intervals. One measure of how good these NMR-based saturation estimates can be is their stability within a given layer of the reservoir. Part of this unvarying behavior is due to the limited vertical resolution of the logging tool, but a large part can be ascribed to the actual measurement results. The observation that NMR-based saturations in the flushed zone obtained with minimal calibration of the results fall within the range of values, 50-75%, generated from imbibition and forced displacement measurements on a wide range of core samples.

Greatest difference in standard S_{xo} and NMR-based saturation estimates occurs in the Upper Ekofisk layers, which in turn results in the significant difference in Archie saturation exponents. Since the Upper Ekofisk interval is believed to be less water-wet than the lower intervals this difference between the two saturation estimates can be explained. The NMR-based saturations reflect water content in the flushed zone, which is undoubtedly affected by viscous displacement mechanisms. In contrast, the core-derived saturation exponents were measured only at spontaneous imbibition endpoints. In highly water-wet intervals the distinction between endpoints is meaningless, but in intervals of reduced water-wetness this distinction becomes critical. This argument reduces to the end-point argument – are values determined from cores measured at imbibition end point sufficient to characterize saturation behavior at the near well-bore that most likely contains a strong forced displacement component? The NMR saturation results suggest that the core-derived exponents are not sufficient to properly characterize S_{xo} values in the reduced water-wet Upper Ekofisk interval.

Acknowledgements

The authors acknowledge permission to publish this paper from Phillips Petroleum Company, Norway and co-venturers, including Fina Exploration Norway S.C.A., Norsk Agip A/S, Elf Petroleum Norge AS, Norsk Hydro Produksjon a.s., TOTAL Norge A.S., Den norsk stats oljeselskap a.s. and Saga Petroleum a.s. Discussions with James Galford lead to the development of the temperature – MRIL porosity correction.

References

- Coates, G.R., Xiao, L., and Prammer, M.G., 1999, *NMR Logging: Principles and Applications*, Halliburton Energy Services, Houston.
- Howard, J.J., Crabtree, B.J., Langley, D.E., Siemers, W.T, and Caldwell, C.D., 1994, "Correlation of laboratory petrophysical measurements to chalk lithofacies and reservoir quality in the greater Ekofisk area", EAPG/AAPG Special Conference on Chalk, Copenhagen, pp. 24-27.
- Howard, J.J. and Spinler, E.A., 1995, "Nuclear magnetic resonance measurements of wettability and fluid saturations in chalk", *SPE Advanced Technology Series*, v. 2.
- Howard, J.J., 1998, "Quantitative estimates of porous media wettability from proton NMR measurements", *Magnetic Resonance Imaging*, v.16, no.5/6, p.529-533.
- Kenyon, W.E., 1997, "Petrophysical principles of applications of NMR logging", *Log Analyst*, v. 38, pp. 21-43.
- Van De Verg, P.E., Howard, J.J., Nesvold, R.L., and Fidan, M., 1999, "Water saturations in breakthrough intervals, Ekofisk Field, Norway", SPWLA 40th Annual Logging Symposium, paper LL, 13pp.